THE ASTROPHYSICAL JOURNAL, 405:L75–L78, 1993 March 10

THE INTERNAL MASS DISTRIBUTION OF A GIANT MOLECULAR CLOUD WITHOUT STAR FORMATION

JONATHAN P. WILLIAMS
Department of Astronomy, University of California, Berkeley, CA 94720
AND
LEO BLITZ
Department of Astronomy, University of Maryland, College Park, MD 20742

Received 1992 December 4; accepted 1992 December 18

ABSTRACT

High-resolution, low-noise maps have been made of Maddalena's cloud, a large, anomalous molecular cloud in which star formation is absent to a very low level. A rich internal structure is observed, despite the apparent lack of energy input. We characterize the structure in terms of clumps and find that the clump mass spectrum is well fit by a power law, $dN/dM \propto M^{-1.0\pm0.16}$, *flatter* than that measured in the same way for the Rosette molecular cloud, a more typical star-forming cloud, and by extrapolation, flatter than the mass spectrum of all giant molecular clouds (GMCs) investigated to date. A Kolmogorov-Smirnov test finds only a 7% probability that the mass distribution of the two clouds sample the same parent distribution. If the clouds that we have observed are not pathological the results suggest that (a) the clumpy structure of molecular clouds is primordial, (b) the mass spectrum of the fragments in a GMC is affected by the evolution of the cloud, and (c) more evolved clouds have a higher fraction of small clumps.

Subject headings: ISM: clouds — ISM: molecules — stars: formation

1. INTRODUCTION

Molecular clouds are the sites of all star formation in the Galaxy. High-mass stars are short lived, yet are observed in all large molecular clouds in the solar neighborhood. These clouds, therefore, are continually forming stars which, in turn, continually feed energy back into the parent molecular material via winds, radiation, and supernovae. Observations of a cloud that is not forming stars are therefore observations of undisturbed cloud structure: the initial conditions for the evolution of clouds into star-forming entities. In this *Letter* we present detailed observations of the structure of such a cloud.

Maddalena & Thaddeus (1985, hereafter MT) reported the discovery of a large, abnormally cold GMC in the outer Galaxy lacking the well-known signs of star formation. The combined absence of associated optical H II regions, strong infrared emission, radio continuum sources, together with low CO temperatures suggests that the cloud is an embryonic GMC in an early evolutionary state prior to star formation. The cloud is not detectable in the *IRAS* sky flux plates at this position (Blitz 1993): the upper limit to the 100 μm luminosity is 5000 $L_\odot$. This is far less than a single O9 star, or in terms of star-formation efficiency, implies an upper limit $\epsilon = M_*/M_{\rm tot} < 0.1\%$.

MT mapped the full extent of the cloud in CO (2°.5 by 1°.8 corresponding to 110 by 80 pc at a kinematic distance of 2.5 kpc), but at insufficient angular resolution and signal-to-noise to be able to detect much fine structure. Detailed observations of molecular clouds have, without exception, found a high degree of internal structure both in position and velocity, most often characterized as "clumps": localized, distinct density maxima, embedded in a low-density interclump gas. The clumps are frequently sites of star formation (e.g., Lada 1990), and as an ensemble show signs of dynamical evolution (Blitz 1993). Clues to cloud evolution, and ultimately star formation, lie in an increased understanding of clump evolution on an individual and collective basis.

In order to analyze the internal structure of this unusual cloud we have recently completed high-resolution, low noise observations in the optically thin ^{13}CO line. A clump finding algorithm has been developed and applied to these data, and also to the Blitz & Stark (1986) observations of the Rosette molecular cloud (hereafter RMC) both as a consistency check on previous results, and as a standard by which to gauge any differences in the Maddalena molecular cloud (MMC). Both are truly GMCs each with luminous masses of several 10^5 $M_\odot$ (the MMC is in fact a few times more massive than the RMC). However, although the RMC has clear signs of past and ongoing high-mass star formation, (Blitz & Thaddeus 1980; Cox, Deharveng, & Leene 1990), the MMC shows none at all. We describe observations of the MMC in § 2, the clump finding algorithm in § 3, with results and discussion in §§ 3 and 4.

2. OBSERVATIONS

We mapped two regions of the MMC with the NRAO 12 m telescope[1] at Kitt Peak, Arizona in the $J = 1 \rightarrow 0$ transition of ^{13}CO during five observing runs from 1990 December to 1992 June. The observations were made using two SIS mixer receivers (one for each polarization) each with total system temperatures in the range 250 to 500 K. Integration times of the position switched observations (reference position $l = 216°.0$, $b = -4°.0$) were adjusted to maintain an approximately uniform rms noise equal to 0.15 K in each of the 250 kHz (0.68 km s^{-1}) wide filters. Pointing was checked using the planets at

[1] The National Radio Astronomy Observatory is operated by Associated Universities, Inc., under cooperative agreement with the National Science Foundation.

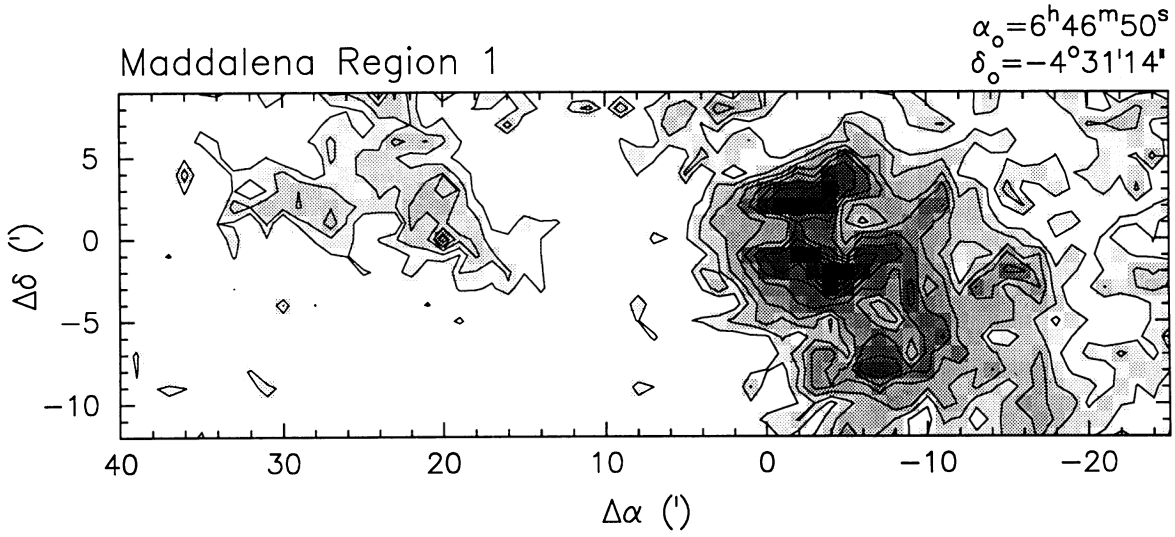

FIG. 1*a*

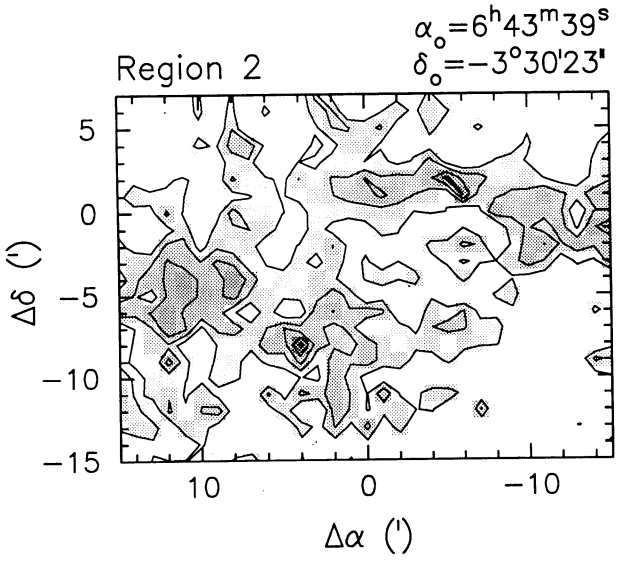

FIG. 1*b*

FIG. 1.—(*a*, *b*) Contour maps and gray scale of ^{13}CO $J = 1 \rightarrow 0$ integrated over the full velocity range of the cloud $v = 15$ to 35 km s^{-1} for each of the mapped regions in Maddalena's cloud. Scales for each axis are offsets in arcminutes in right ascension and declination from zero point $\alpha = \alpha_0$, $\delta = \delta_0$ defined at the top right corner. Contour intervals are 1 K km s^{-1}, beginning at 2 K km s^{-1}.

the beginning, middle and end of each observing session, and rms pointing accuracies were generally better than 10″. Overall calibration was checked daily using standard positions in the nearby Orion and Rosette molecular clouds and antenna temperatures are accurate to 15%. Scaling of data between different observing runs was only necessary on the last run when a 20% (upward) correction was made. Baselines were consistently flat, a first order fit was always sufficient.

Map spacing for each of the two regions is 1′, the telescope beamwidth. We were particularly interested in making a comparison with the ^{13}CO data for the RMC. The ratio between the beamwidths of the 12 m telescope we used to map the MMC and the 7 m Bell Laboratories telescope that Blitz & Stark (1986) used to map the RMC is nearly equal to the ratio of the distances to each cloud, thus the linear resolution of the two sets of observations is nearly identical. Moreover, the velocity resolution is exactly the same for each cloud since 250 kHz filter banks were used for both sets of observations. A beam efficiency correction ($\eta_{fss} = 0.9$, Kutner & Ulich 1981) has been applied to the 7 m data so that temperatures for each cloud are T_R^*. Whereas more than 50% of the RMC was mapped in ^{13}CO, observing time limitations and the smaller beam size restricted mapping of the MMC to less than 10% of its larger total area. However because the mapped area of each cloud in pc^2 is similar, the two data sets can be directly compared.

Velocity integrated maps of each region are displayed in Figures 1*a* and 1*b*. Region 1 was centered on the brightest point in the CO map of MT, whereas Region 2, about 1°.5 away, was selected to be a more typical location to ensure that the limited subsample of the cloud that we observed is representative of the cloud as a whole.

3. THE CLUMP-FINDING ALGORITHM

Figure 2 is a position-velocity ($\alpha - v$) map of the first region which demonstrates that the observations successfully reveal detailed internal structure in the MMC. Although several clumps are easily identified by eye in this diagram, the task of following them and their mergers through neighboring slices, i.e., describing the clumpy structure in three dimensions, quickly becomes very complex. This has, however, been the method by which the majority of clouds have been studied to date (see Blitz 1993, and references therein). In order to facilitate unbiased comparisons between different clouds, we were motivated to develop a reliable, automatic clump-finding algorithm.

A full description and testing of the algorithm is given in Williams, de Geus, & Blitz (1993). We briefly describe it here. The primary difficulty in devising an automatic algorithm is that one is attempting to derive physical quantities about discrete clumps from maps in which the clump emission is blended. Finding a reliable way to assign the blended emission to each of the contributing clumps is the crux of the problem. For a two-dimensional contour map it is a simple matter to pick out peaks and their associated regions; similarly one can imagine peaks in a position-position-velocity data cube surrounded by "surfaces" defined by a set of intensity levels (three-dimensional contours). Peaks that share a common surface are blended. The method used here essentially identifies clumps from the unblended emission and then assigns the

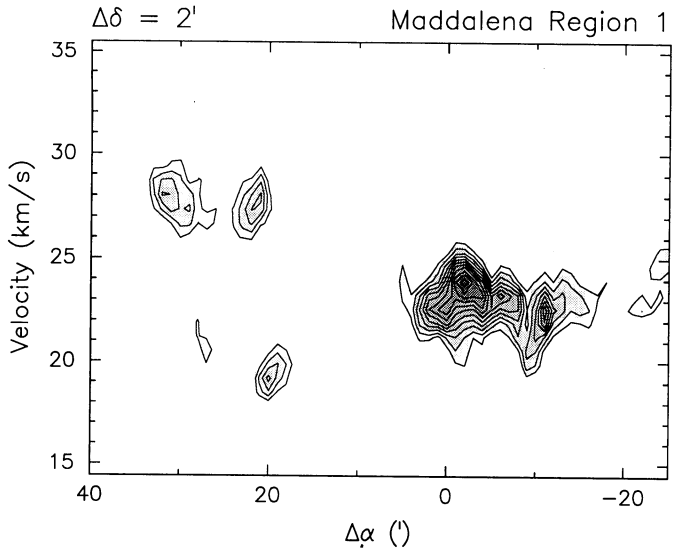

FIG. 2.—Position-Velocity map of a slice along $\Delta\delta = 2'$ in region 1. Contours start at 0.5 K and increment 0.25 K each level.

emission from blended regions to various contributing clumps in a well defined way.

In an optically thin tracer, local maxima in the data cube correspond to real density enhancements, i.e., clumps. Our procedure assumes that each clump is identified by a local maximum in the cube; the number of clumps is *determined* by the number of local maxima. As we follow clumps to lower intensity levels, blending of emission from neighboring clumps will occur. For the case of moderate signal-to-noise and resolution the unblended region surrounding the peak of a clump is sufficient to make a good estimate of its size. The stronger the peak and the wider the clump, the greater its contribution to nearby blended regions. By considering each clump's position, intensity, and size, we can estimate the *relative* contribution of each clump at each point in the data cube and reassign each one an equivalent proportion of the observed intensity. We iterate this procedure until changes in the clump parameters are small.

Any extrapolation into the blended areas of emission necessarily assumes some profile, or shape, of the clumps. The effect of this assumption is minimized by using it only to assign *relative* proportions of the observed intensity, and by fixing the number of clumps at the start (equal to the number of local maxima in the map).

To handle the practical case of a discrete grid of data points and noise, parameters describing the contour level increments, and resolution of the surfaces are introduced. By creating simulated data and comparing the output of the algorithm with the input, we can evaluate the effect of discreteness and noise in the data and find optimum values of the parameters that maximize how well the output list of clump parameters match the input list. The simulations show that the algorithm is robust and reliably handles a diverse variety of realistic data. As a final check we have also verified that the clumps identified by the algorithm agree well with what one picks out by eye.

4. RESULTS

In this *Letter* we report only the mass spectrum of the clumps found for each cloud: a more thorough description of the clump properties will be given in a subsequent paper. In calculating the clump masses we must convert from integrated temperatures to hydrogen column densities: we assume small optical depth, and constant excitation temperature across the cloud, estimated from CO observations to be 20 K for the RMC and 10 K for the MMC. An LTE correction is applied and we convert to H_2 column density assuming $N_{H_2}/N_{^{13}CO} = 4.8 \times 10^5$ (see Bertoldi & McKee 1991 for discussion). We take the same conversion for both clouds as suggested by the star count measurements of the MMC by Lee, Snell, & Dickman (1991). Masses are then multiplied by 1.4 to account for helium (10% by number).

The mass spectra are presented in Figures 3*a* and 3*b*. We have assumed errors for each bin equal to $N^{1/2}$ where N is the number of clumps in any mass bin, and have fit the binned data with a power law of the form $dN/dM \propto M^{-\alpha}$. For the RMC we find $\alpha = 1.24 \pm 0.12$, and for the combined clump data from both mapped regions in the MMC $\alpha = 0.99 \pm 0.16$, significantly flatter than the RMC. In each case we have not included

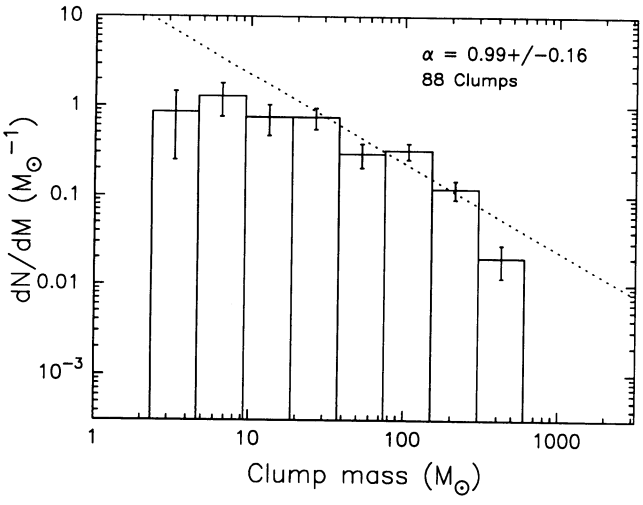

FIG. 3*a*

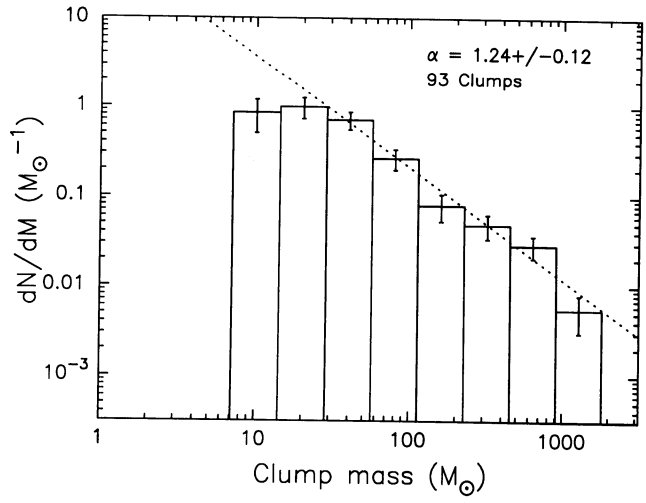

FIG. 3*b*

FIG. 3.—Clump mass spectra of the (*a*) Maddalena and (*b*) Rosette clouds. Clumps have been derived in the same manner for each cloud using the algorithm described in the text. Abscissa is the clump mass in solar units derived from the ^{13}CO luminosity. Ordinate is the number of clumps in each mass bin ΔN [with errors $\pm(\Delta N)^{1/2}$], divided by the width of the mass bin ΔM, which is the clump mass spectrum dN/dM. Both axes are logarithmic and the histogram is fit by a straight line in each case corresponding to a power-law form $dN/dM \propto M^{-\alpha}$ where $-\alpha$ is the slope of the fitted line. For the MMC, the lowest three mass bins are not included in the fit, for the RMC the lowest two.

mass bins below the 20 $M_\odot$ bin in the fit. We have chosen contour intervals (0.5 K for the RMC, and 0.25 K for the MMC) at about twice the noise, implying a minimum mass detectability $M_{d,\mathrm{RMC}} \sim 8\ M_\odot$ and $M_{d,\mathrm{MMC}} \sim 3\ M_\odot$. Although we do detect clumps of mass $M \sim M_d$, the mass spectra are only complete at $M \sim O(3\text{–}4)M_d$. Our simulations confirm this result and appears to be due to the noise which has a greater relative effect on the smaller clumps because of their lower temperatures. We have also calculated the mass spectrum for each of the two mapped regions in the MMC individually, and they are not significantly different from one another.

It is also possible to make a direct cloud-to-cloud comparison without binning the data and fitting to a power law. For each cloud and associated clump list we calculate the proportion of clumps below a mass M (the cumulative distribution function) as a function of M, and in Figure 4 we plot the difference between them. For $M \lesssim 100\ M_\odot$ the difference is positive indicating that there are proportionally more small mass clumps in the RMC than in the MMC, but the reversal at $M \sim 100\ M_\odot$ shows that the mass spectrum for the MMC is flatter and has proportionally more larger mass clumps. The maximum deviation from zero is used to determine the Kolmogorov-Smirnov likelihood (Press et al. 1992) that the clumps for each cloud do indeed share the same mass distribution. The value of 7% would suggest that they do not.

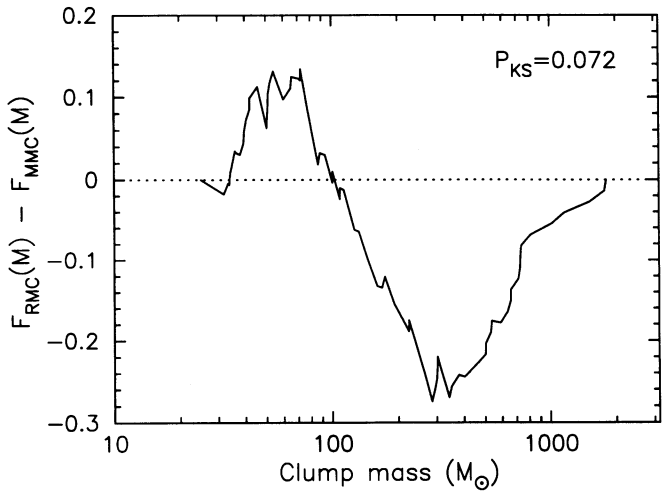

FIG. 4.—Direct comparison of the RMC and MMC using the Kolmogorov-Smirnov statistic. Plotted is the difference between the cumulative distribution function $F(M)$ between each cloud against the clump mass. Here $F(M)$ is the proportion from zero to one of the number of clumps with mass less than M. The maximum deviation from zero gives a likelihood of only 7% that the two clouds share a common mass distribution.

5. DISCUSSION

The MMC is a very large and unusual molecular cloud that is not forming stars at present; the simplest interpretation is that it is a young version of more typical star-forming clouds such as Orion and the Rosette. We first note that despite the lack of star formation, we have observed a high degree of internal structure and can clearly identify many clumps. The clumpy structure is therefore primordial, and not due to the presence of stars. Subsequent star formation may modify the clumps but does not directly create them.

Clumps have been identified, catalogued, and their masses determined for both the Maddalena and Rosette molecular clouds. We have used different excitation temperatures for each cloud as indicated by CO observations. This can affect mass estimates, but not the *slope* of the mass spectrum. In all other respects the two data sets are directly comparable and have been analyzed in the same way so selection bias differences between the two are minimal. We note that the algorithm calculates a somewhat shallower mass spectrum for the RMC than the result quoted by Blitz (1986, 1993).

Mass spectra of a number of star forming clouds have been previously determined (Nozawa et al. 1991; Lada, Bally, & Stark 1991; Carr 1987; Stutzki & Güsten 1990; Loren 1989). Clump masses from a few to several thousand solar masses have been observed, and in each cloud the mass spectrum power law index has a value close to -1.5. The MMC result presented here is the only case so far with a significantly different clump mass spectrum. The deviation is in the sense that the total cloud mass is more strongly concentrated in the more massive clumps in the MMC indicating that clump evolution is predominantly one of fragmentation (possibly as a result of collisions), rather than agglomeration. Unless there is a hitherto unknown class of GMCs that simply does not *ever* form high-mass stars, it is inevitable that such a massive cloud will eventually evolve to become more like the RMC and other star forming clouds that have been observed (McKee & Williams 1993).

The discovery of a GMC without star formation is an important find for understanding the initial conditions and the embryonic internal structure of a cloud undisturbed by stellar processes. We have made high-resolution observations of such a GMC and find that in at least one characterization of the clump ensemble—the clump mass spectrum—there is a significant difference compared to star forming molecular clouds. If our results are generally applicable, they imply that the clump mass spectrum is an indicator of the evolutionary state of a GMC. If the MMC is destined to form stars and to possess a mass spectrum typical of such objects then the cloud mass must predominantly fragment into smaller clumps than agglomerate into more massive clumps.

This work is partially funded by AST89-18912. The authors thank Eugène de Geus for many helpful discussions concerning the clump finding algorithm, and the referee, Charlie Lada for his careful reading of the manuscript.

REFERENCES

Bertoldi, F., & McKee, C. F. 1991, ApJ, 395, 140
Blitz, L. 1986, in Physical Processes in Interstellar Clouds, ed. G. E. Morfill & M. Scholer (Dordrecht: Kluwer), 35
———. 1993, in Protostars and Planets III, ed. E. H. Levy & J. I. Lunine (Tucson: Univ. Arizona Press), in press
Blitz, L., & Stark, A. A. 1986, ApJ, 300, L89
Blitz, L., & Thaddeus, P. 1980, ApJ, 241, 676
Carr, J. S. 1987, ApJ, 323, 170
Cox, P., Deharveng, L., & Leene, A. 1990, A&A, 230, 694
Kutner, M. L., & Ulich, B. L. 1981, ApJ, 250, 341
Lada, E. A. 1990, Ph.D. thesis, Univ. Texas
Lada, E. A., Bally, J., & Stark, A. A. 1991, ApJ, 368, 432
Lee, Y., Snell, R. L., & Dickman, R. L. 1991, ApJ, 379, 639
Loren, R. B. 1989, ApJ, 338, 902
Maddalena, R., & Thaddeus, P. 1985, ApJ, 294, 231 (MT)
McKee, C. F., & Williams, J. P. 1993, in Star-Forming Galaxies and their Interstellar Medium, ed. J. J. Franco (Cambridge: Cambridge Univ. Press), in press
Nozawa, S., Mizuno, A., Teshima, Y., Ogawa, A., & Fukui, Y. 1991, ApJS, 77, 647
Press, W. H., Teukolsky, S. A., Vetterling, W. T., & Flannery, B. P. 1992, Numerical Recipes, (Cambridge: Cambridge Univ. Press)
Stutzki, J., & Güsten, R. 1990, ApJ, 356, 513
Williams, J. P., de Geus, E. J., & Blitz, L. 1993, in preparation